In the Trenches of Real-World Self-Control : Neural Correlates of Breaking the Link Between Craving and Smoking

Elliot T. Berkman, Emily B. Falk and Matthew D. Lieberman

Psychological Science published online 4 March 2011
DOI: 10.1177/0956797611400918

Psychological Science OnlineFirst, published on March 4, 2011 as doi:10.1177/0956797611400918

Research Article

Psychological Science
XX(X) 1–9

DOI: 10.1177/0956797611400918
http://pss.sagepub.com

In the Trenches of Real-World Self-Control: Neural Correlates of Breaking the Link Between Craving and Smoking

Elliot T. Berkman[1], Emily B. Falk[2], and Matthew D. Lieberman[3]
[1]University of Oregon, [2]University of Michigan, and [3]University of California, Los Angeles

Abstract

Successful goal pursuit involves repeatedly engaging self-control against temptations or distractions that arise along the way. Laboratory studies have identified the brain systems recruited during isolated instances of self-control, and ecological studies have linked self-control capacity to goal outcomes. However, no study has identified the neural systems of everyday self-control during long-term goal pursuit. The present study integrated neuroimaging and experience-sampling methods to investigate the brain systems of successful self-control among smokers attempting to quit. A sample of 27 cigarette smokers completed a go/no-go task during functional magnetic resonance imaging before they attempted to quit smoking and then reported everyday self-control using experience sampling eight times daily for 3 weeks while they attempted to quit. Increased activation in right inferior frontal gyrus, pre-supplementary motor area, and basal ganglia regions of interest during response inhibition at baseline was associated with an attenuated association between cravings and subsequent smoking. These findings support the ecological validity of neurocognitive tasks as indices of everyday response inhibition.

Keywords

self-control, smoking cessation, brain-as-predictor, right inferior frontal gyrus, response inhibition, text messaging

Received 9/21/10; Revision accepted 10/22/10

Ridding oneself of an unwanted habit or tendency is a war that consists of a series of momentary self-control skirmishes. A longtime smoker may decide to quit, but success in reaching that goal will depend on the individual outcomes of a series of battles with cigarette cravings. Understanding the neural processes involved in these brief repeated struggles, in smoking and in other domains, is essential to understanding how self-control works in the trenches of real-world goal pursuit. The investigation reported here focused on response inhibition as one key factor that influences the ultimate success or failure of goal pursuit, and overcoming addiction in particular. Behavioral studies have examined how response inhibition during lab-based tasks relates to general real-world success at overriding an unwanted habitual behavior in favor of a desired novel one (Wood & Neal, 2007). Similarly, cognitive neuroscience studies have examined the neural correlates of response inhibition in the lab. However, because of limitations inherent to these two methods, no study has identified the neural systems that support effective response inhibition during the brief and repeated self-control episodes in daily life that are integral to successful long-term goal pursuit. In the current study, we investigated this question using a novel integration of methods, combining within-scanner measures of response inhibition with assessment of daily, momentary self-control along the way to a larger habit-changing goal.

Behavioral performance on simple laboratory response-inhibition tasks (e.g., go/no-go) has been consistently linked to success in reaching a variety of real-world goals that involve self-regulation. For instance, the capacity to engage response inhibition has been linked to success at dieting (Rothman, Sheeran, & Wood, 2009), increased exercise (Achtziger, Gollwitzer, & Sheeran, 2008), and improved academic competency (Oaten & Cheng, 2006). Conversely, diminished response-inhibition capacity has been linked to alcoholism (Nigg et al., 2006), methamphetamine abuse (Monterosso, Aron, Cordova, Xu, & London, 2005), and even domestic violence (Finkel, DeWall, Slotter, Oaten, & Foshee, 2009). These studies have demonstrated a robust association between behavioral performance on simple behavioral tasks assessing

Corresponding Author:
Elliot T. Berkman, Department of Psychology, University of Oregon, 1227 University of Oregon, Eugene, OR 97403-1227
E-mail: berkman@uoregon.edu

response inhibition and important real-world outcomes, but have not focused specifically on the brief and repeated instances of self-control that occur as part of goal pursuit and collectively contribute to long-term success.

Neuroscience studies have converged in identifying a consistent network of brain regions that are active during brief, laboratory-based manipulations of response inhibition. A number of functional neuroimaging (Aron, Robbins, & Poldrack, 2004; Leung & Cai, 2007) and lesion (Aron, Fletcher, Bullmore, Sahakian, & Robbins, 2003; Chambers et al., 2006) studies have implicated the right inferior frontal gyrus (rIFG) as the primary brain region for response inhibition. Many studies have also found that the dorsal anterior cingulate cortex (dACC), the anterior insula, the pre-supplementary motor area (pre-SMA), and subcortical regions such as the basal ganglia are coactive with the rIFG during response inhibition (Aron et al., 2007; Wager et al., 2005). Though the precise role of each of these regions in the human response-inhibition network is unclear, recent studies have suggested that the pre-SMA and dACC are involved in detection of potential conflict between the prepotent and desired response (Botvinick, Cohen, & Carter, 2004; Mostofsky & Simmonds, 2008; Nachev, Wydell, O'Neill, Husain, & Kennard, 2007), the rIFG plays a role in representing the mapping between the inhibition cue and stopping (Van Gaal, Ridderinkhof, Scholte, & Lamme, 2010), and the subcortical structures are important for directly inhibiting the motor response (Aron et al., 2007). These explanations fit well into the broader view that the prefrontal cortex executes top-down control via a neuroanatomical control loop including the basal ganglia and primary and supplementary motor areas (Fuster, 2008). These studies characterize the brain networks involved in response inhibition at a single point in time, but do not capture the repeated and motivationally relevant nature of response inhibition during real-world goal pursuit.

Thus, on one hand, behavioral measures of response inhibition have been associated with a broad array of real-world outcomes, such as prevention of addiction relapse. On the other hand, the brain systems recruited for inhibiting responses during brief laboratory tasks are being mapped with increasing precision. Juxtaposing the behavioral and neuroscience literatures on response inhibition highlights why the neural processes underlying real-world instances of response inhibition have remained unexplored. There is almost no overlap between these literatures beyond similarity in the tasks used to assess response inhibition. Consequently, it is unknown whether the neural systems involved in laboratory assessments of response inhibition are the same ones recruited in the brief and repeated everyday battles between habit and self-control. For example, it is possible that the neural systems recruited during the stop-signal task are different from those associated with increasing exercise. Linking these disparate levels of analysis (i.e., neural and social/behavioral) and time scales (i.e., seconds/minutes and days/weeks) requires a paradigm for examining response inhibition during real-life situations and also during neuroimaging tasks in the same sample of individuals.

Accordingly, we made this link by measuring the neural mechanisms and everyday implementation of response inhibition within a single study. We recruited a sample of individuals just before they were to engage in the long-term, real-life response-inhibition task of quitting cigarette smoking and used functional MRI (fMRI) to examine their neural activation during a laboratory response-inhibition task. Next, we used experience sampling to track their progress throughout each day for the first 3 weeks of their smoking-cessation attempt (Fig. 1). Brain data in a priori regions of interest were then used to predict successful craving regulation on a daily basis during smoking cessation. This approach allowed us to test whether, and how, response-inhibition-related neural activation during the laboratory task related to response inhibition in the real world. We hypothesized that activation in the brain regions thought to be the most directly involved in inhibiting a motor response—the rIFG, pre-SMA, and basal ganglia—would predict successful regulation of daily craving.

Method

Participants

Thirty-one participants (15 female, 16 male) were recruited from smoking-cessation programs in Los Angeles via in-person announcements at orientation sessions. All participants were heavy smokers (> 10 cigarettes/day, 7 days/week, for at least 1 year and urinary cotinine > 1,000 ng/mL) enrolled in a professionally led cessation program (e.g., Freedom From Smoking). To be included in the study, participants also were required to have a score of 9 or 10 (out of 10) on the Contemplation Ladder, a single-item measure of intentions to quit (Biener & Abrams, 1991), and a cumulative score of at least 18 (out of 20) on the Action subscale of the Readiness to Change Questionnaire (Rollnick, Heather, Gold, & Hall, 1992), a four-item measure of the action stage of change. Participants ranged in age from 28 to 69 years (M = 46, SD = 9.7) and had smoked for 11 to 53 years (M = 28.4, SD = 2.0). The sample was 52% Caucasian, 26% Hispanic, 19% African American, and 3% other ethnicities. Participants were excluded if they were left-handed, did not speak English, consumed more than 10 alcoholic drinks per week, or had any of the following conditions: dependence on substances other than nicotine at the time of study, dependence on substances within the previous year, neurological or psychiatric disorders, cardiovascular disease, pregnancy, claustrophobia, or any other condition contraindicated for MRI.

Of the original 31 participants, all completed the scanning session, but 1 withdrew from participation in the experience-sampling phase, and 3 were excluded for insufficient data; thus, 27 participants were included in the analyses reported here. Participants were compensated $80 for completing the scanning session and an additional $1 for each experience-sampling response returned, for a possible total of $248. All participants provided written informed consent approved by the UCLA Institutional Review Board.

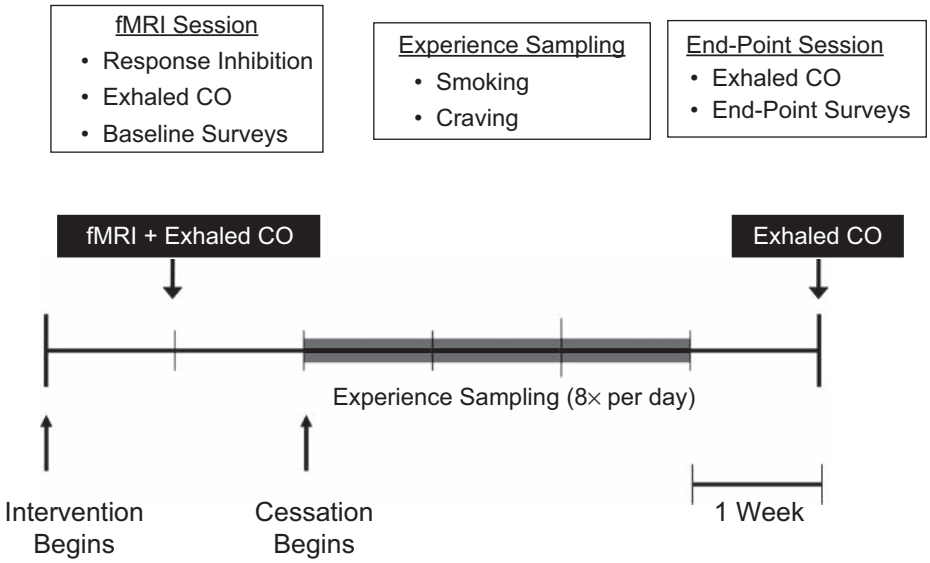

Fig. 1. Timeline of the experiment. The baseline (scanning) session occurred following registration in a smoking-cessation program but prior to smoking reduction. During this session, participants performed the functional MRI (fMRI) response-inhibition (go/no-go) task and completed baseline measures of self-reported smoking; exhaled carbon dioxide (CO) was also measured. The experience-sampling phase began the day prior to the targeted quit date and continued for 21 consecutive days. Participants reported smoking and cravings at eight time points that were evenly spaced between wake-up time and bedtime. During the end-point session, which occurred approximately 4 weeks following the targeted quit date, additional surveys were administered, and exhaled CO was measured.

Procedure

Phone screening. Following recruitment, participants were contacted by telephone to assess their intentions to quit (with the Contemplation Ladder and Readiness to Change Questionnaire) and their targeted quit date (TQD), as well as whether they met any of the exclusion criteria. For qualifying participants, a baseline laboratory session was scheduled at least 1 day prior to the TQD.

Baseline (scanning) session. Participants came to the UCLA Ahmanson-Lovelace Brainmapping Center for a baseline session at least 1 day prior to their quit date (Fig. 1). After they provided written informed consent, their smoking status was confirmed with a urinary cotinine assay (Accutest NicAlert strips; JANT Pharmacal Corp., Encino, CA), and baseline exhaled carbon monoxide (CO) was measured (Micro-smokerlyzer; Bedfont Scientific Ltd., Kent, United Kingdom). Participants were screened for amphetamines, cocaine, marijuana, opiates, and PCP via urine test (Syva RapidTest d.a.u. 5; Dade Behring Inc., Cupertino, CA).

We used a go/no-go task to examine the neural activation associated with response inhibition (Fig. 2). The task consisted of 12 blocks containing a series of brief trials, each depicting a single letter centered in the screen. Each block began with the instruction to "push" or to "pull" the joystick lever. Then, depending on which instruction was given, participants pushed or pulled the lever whenever the letter *L*, *N*, *T*, or *V* appeared (go trials; ~82% frequency) and withheld a response when the letter *X* appeared (no-go trials; ~18% frequency). A neural measure of response inhibition was defined as the difference between brain activation during successful no-go trials (overriding the prepotent "go" response) and brain activation during go trials in an event-related analysis. Each block contained an average of 9 no-go trials and 41 go trials, and each trial lasted 1 s. The intertrial interval (ITI) was jittered according to a random gamma distribution ($M = 0.5$ s). Each block (50 trials and ITIs) lasted 75 s, and blocks were separated by 12-s rest periods. The blocks were divided across four fMRI runs.

After completing this task, participants were removed from the scanner and brought into a quiet testing room for the duration of the session. Participants completed measures of demographics, smoking history, waking hours, nicotine dependence (Fagerström Test of Nicotine Dependence; Heatherton, Kozlowski, Frecker, & Fagerström, 1991), and smoking urges (Questionnaire on Smoking Urges; Tiffany & Drobes, 1991), in addition to several other questionnaires not relevant to the hypotheses tested here. Participants who did not have or preferred not to use their own cell phones were provided with and instructed to use a prepaid phone. Finally, participants were instructed in the use of text messages to receive and respond to experience-sampling prompts, and successfully completed a practice prompt.

Experience sampling. Following the scanning session, and beginning 1 day prior to their quit date, participants received prompts via text message eight times per day for 21 consecutive days. The first text prompt on each day was sent 15 min

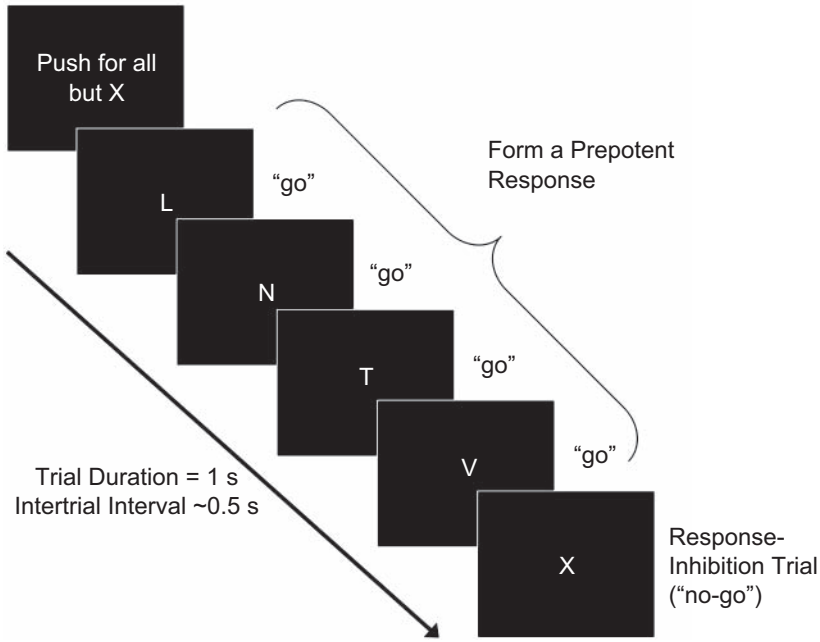

Fig. 2. The go/no-go task. Participants responded using the lever whenever the letter *L*, *N*, *T*, or *V* appeared (go trials) and withheld a response when the letter *X* appeared (no-go trials). In an event-related analysis, a neural measure of response inhibition was defined as the difference between brain activation during successful no-go trials (overriding the prepotent "go" response) and brain activation during go trials. Each of 12 blocks contained fifty 1-s trials (~41 go trials and ~9 no-go trials) separated by gamma-distributed jitter (*M* = 0.5 s).

after morning rise, the last prompt was sent 15 min before bedtime, and the other six were evenly distributed throughout the day. Rise times and bedtimes were adjusted for each participant for weekdays and weekends. The interprompt interval varied across subjects between 1 hr 50 m and 2 hr 25 m.

At each prompt, participants responded to three questions: "How many cigarettes have you smoked since the previous signal?" (numerical response), "How much are you craving a cigarette right now?" (0 = *not at all*, 1 = *a little*, 2 = *somewhat*, 3 = *a lot*, 4 = *extremely*), and "Overall, how is your mood right now?" (0 = *extremely negative*, 1 = *somewhat negative*, 2 = *neutral*, 3 = *somewhat positive*, 4 = *extremely positive*). Participants responded to all three questions with a single text message back to the experimenters. See the Supplemental Text (Supplementary Methods) in the Supplemental Material available online for further details.

End-point session. An end-point session was scheduled within 7 days of the end of the 21-day experience-sampling period. Exhaled CO was reassessed along with nicotine dependence (Fagerström Test of Nicotine Dependence) and smoking urges (Questionnaire on Smoking Urges). Participants were compensated $1 for each text-message response (*M* = $141, *SD* = $38).

fMRI data acquisition and analysis

Brain-imaging data were acquired on a 3-T Siemens Trio scanner at the UCLA Ahmanson-Lovelace Brainmapping Center using standard data-acquisition and preprocessing steps (see the Supplemental Text in the Supplemental Material). The main effect of response inhibition was defined using a linear contrast for each participant (i.e., no-go > go). Contrast images were averaged across runs for each participant and then entered into a random-effects analysis at the group level. We constructed regions of interest (ROIs; Fig. 3) for the rIFG (pars triangularis, pars orbitalis, and pars opercularis; Aron et al., 2004), basal ganglia (encompassing caudate, putamen, and globus pallidus; Williams et al., 2006), and pre-SMA ($y > 0$; Aron & Poldrack, 2006) using the Automated Anatomical Labeling (AAL) toolbox (Tzourio-Mazoyer et al., 2002) within the Wake Forest University Pickatlas (Maldjian, Laurienti, Kraft, & Burdette, 2003). Also using AAL, we constructed control ROIs for discriminant validity in the bilateral precuneus and amygdala. These regions were chosen to represent one cortical and one subcortical region for which activation is often observed in cognitive neuroscience tasks but not typically during response inhibition. Analyses based on ROIs used a two-tailed significance threshold of .05.

Experience-sampling data-analysis strategy

Multilevel linear modeling was used to address the nested nature of the experience-sampling data (HLM 6; Scientific Software International, Lincolnwood, IL; Raudenbush, Bryk, Cheong, & Congdon, 2004). A three-level model was

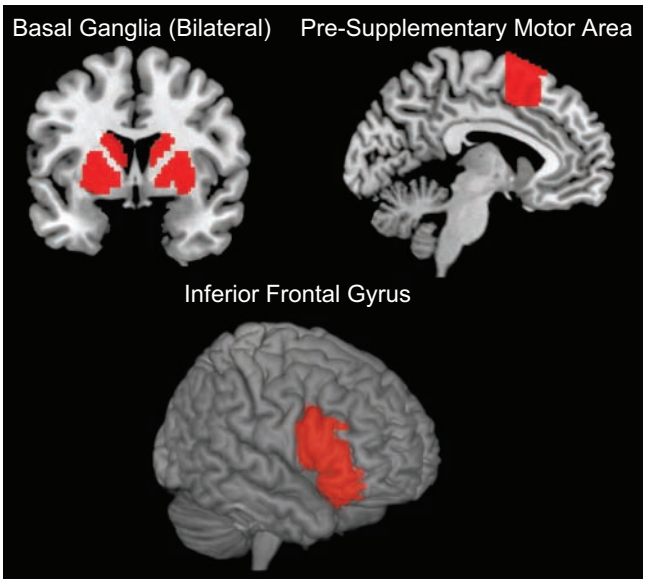

Fig. 3. The a priori anatomical target regions of interest from the Automated Anatomical Labeling (AAL) atlas (Tzourio-Mazoyer et al., 2002). The basal ganglia comprised the caudate, putamen, and globus pallidus; the pre-supplementary motor area was defined using the AAL and was restricted to be anterior to the anterior commissure (i.e., Montreal Neurological Institute *y* coordinates > 0); and the right inferior frontal gyrus was defined according to the AAL pars opercularis, triangularis, and orbitalis.

constructed with time points (Level 1) nested within days (Level 2) nested within participants (Level 3). This model allowed us to examine the time-lagged relationship between craving and smoking within days while accounting for the nested structure of the data. The primary dependent measure of smoking was nonnormally distributed because it was reported as a count at each time point. Accordingly, we used a Poisson model with a log link function at the first level. Thus, all parameters are reported in log-expected likelihood units. Significance values were calculated using estimates of standard errors that are robust to violations of sphericity (see Supplemental Text in the Supplemental Material).

Integration of fMRI and experience-sampling data

To assess everyday response inhibition, we estimated the prospective relationship between craving for a cigarette at one time point and smoking at the subsequent time point. The magnitude of the relationship between these measures provided an ecological measure of response inhibition because cravings are among the primary impulses that must be regulated in successful smoking cessation (Allen, Bade, Hatsukami, & Center, 2008; Shiffman et al., 1997). To assess the relationship between laboratory neural and real-world behavioral measures of response inhibition, we imported neural activation parameters from the fMRI task into the HLM model as a person-level (Level 3) moderator of the slope between past craving and subsequent smoking. We entered three anatomically defined ROIs (rIFG, basal ganglia, and pre-SMA; Fig. 3) into separate analyses because they were multicollinear during the contrast of interest (no-go > go). The two control ROIs (amygdala and precuneus) were also entered separately for discriminant validity. Finally, we completed an exploratory whole-brain search for regions that predicted smoking reductions and subjected these results to a cross-validation analysis (see Supplemental Text in the Supplemental Material).

Results

Behavioral responses to the go/no-go task

Participants completed 108 no-go and 492 go trials across 12 go/no-go blocks. The error rate on no-go trials was 4.6%. Error trials were included in the model but not examined because of insufficient *N*. The mean response time on go trials was 547.9 ms (SD = 160.5).

Experience-sampling response rates

Participants responded to 84% of the prompts during the experience-sampling phase of the study (~6.7 responses out of 8 prompts daily). Most responses were sent within 23 min of the signal (SD = 44 min). For a given participant, a day was excluded if it contained fewer than four responses. In total, 90 days were excluded (M = 3.33 per participant). Robustness analyses suggest that the missing data did not affect the results (see Supplemental Text in the Supplemental Material). There were a total of 3,811 Level 1 observations (time points within days), 477 Level 2 observations (days within participants), and 27 Level 3 observations (participants) in our multilevel model.

Smoking and craving during experience sampling

Participants smoked 20.2 cigarettes per day (SD = 9.4) at baseline and 5.2 cigarettes per day (SD = 5.4) at the end point (mean change = 15.0), $t(26) = 7.62$, $p < .01$. Nicotine dependence and urges also decreased significantly (Table 1). Exhaled CO was marginally reduced, $t(26) = 1.94$, $p = .06$ (Table 1). The relatively high rate of lapse is common for smokers in the early weeks of a quitting attempt (Shiffman et al., 2007).

There was a positive within-day relationship between craving at one time point and smoking at the next when craving was entered alone into the model (i.e., without neural activations; log-expectation $\gamma = .19$, $SE = .08$), $t(476) = 2.14$, $p < .05$. Reductions in the number of cigarettes smoked per day were inversely related to the daily craving-smoking link (see

Table 1. Mean Change on Smoking-Related Measures

Measure	Baseline	End Point	Change
Global smoking self-report (no. cigarettes/day)	20.24 (9.36)	5.17 (5.45)	15.07** (10.28)
Exhaled carbon monoxide	18.93 (11.65)	13.44 (10.89)	5.49† (14.70)
FTND	6.37 (2.04)	2.63 (2.62)	3.74** (2.49)
QSU: positive smoking urges	4.82 (1.18)	2.54 (1.57)	2.28** (1.50)
QSU: negative smoking urges	3.24 (1.21)	2.00 (0.97)	1.24** (1.35)

Note: Standard deviations are given in parentheses. $N = 27$. FTND = Fagerström Test of Nicotine Dependence (Heatherton, Kozlowski, Frecker, & Fagerström, 1991); QSU = Questionnaire on Smoking Urges (Tiffany & Drobes, 1991).
†$p = .06$. **$p < .01$.

Supplemental Text in the Supplemental Material for analysis of the relationship between the craving-smoking slope and smoking reductions).

Predicting everyday response inhibition from neuroimaging data

To examine the association between neural activation at baseline and longitudinal outcomes, we extracted activations from the no-go > go contrast for anatomically defined ROIs in the IFG, basal ganglia, and pre-SMA (Fig. 3), as well as the precuneus and amygdala control ROIs (all bilaterally). These activations were used as moderators of the within-day relationship between craving at time i and smoking at time $i + 1$. As in prior research (e.g., Wager et al., 2005), all target regions were significantly more active during no-go than during go trials (all ps < .01, corrected for multiple comparisons) and none of the control ROIs were differentially active (all ps > .2). Because of multicollinearity among the target ROIs (all rs > .6, all ps < .01), each ROI was entered into its own model with no other neural predictors. All models controlled for the linear decline in smoking across days, a quadratic pattern within days (increased smoking in the afternoon and evening compared with the morning), and baseline nicotine dependence. The results remained unchanged with age entered as a covariate.

There was an overall positive relationship between craving at time i and smoking at time $i + 1$. The IFG, basal ganglia, and pre-SMA ROIs each significantly and negatively moderated that slope (Table 2); greater activity in these regions during the laboratory inhibition task related to attenuation of the link between craving and subsequent smoking in the real world. Though cravings were followed by increased smoking on average, participants who showed more inhibition-related activation in the target ROIs at baseline showed less coupling between cravings and later smoking. The moderating effect for the rIFG ROI is depicted in Figure 4, which indicates that individuals with low activation in rIFG (1 *SD* below the mean) in the no-go > go contrast showed a strong positive relationship between cravings and subsequent smoking, simple slope (log units) = 0.53, $t(25) = 2.79$, $p < .01$ (calculation following Bauer & Curran, 2005). Individuals at the mean showed a modest positive (though nonsignificant) relationship, simple slope (log units) = 0.25, $t(25) = 1.20$, n.s., and individuals with high activation (1 *SD* above the mean) showed no relationship between craving and smoking, simple slope (log units) = −0.04, $t(25) = 0.21$, n.s. In other words, an individual with average cravings on an average day would be expected to decrease his or her smoking by 33.6% for each standard deviation increase in rIFG activation during response inhibition at baseline; this translates to an increase of 4.48 cigarettes per day for the average subject. Within the basal ganglia ROI, activation in bilateral putamen and left caudate significantly moderated the craving-smoking link (see Supplemental Text in the Supplemental Material for details). Activity in right amygdala (a control ROI) positively moderated the relationship, such that individuals with higher right amygdala activation during response inhibition at baseline were more likely to smoke given high prior cravings (Table 2). None of the other control ROIs was a significant moderator of the craving-smoking link.

We also examined the relationship between activity in each ROI and long-term cessation success (i.e., across 4 weeks). Only activity in basal ganglia, and not in the other two ROIs, predicted long-term reductions in smoking as measured by change in exhaled CO (Montreal Neurological Institute coordinates: $x = 30$, $y = 5$, $z = 4$; 86-voxel extent, $t = 5.02$, false-detection-rate-corrected $p < .05$; see Supplemental Text, Table S1, and Fig. S1 in the Supplemental Material). This result was further supported by a predictive cross-validation analysis (see Fig. S2 in the Supplemental Material).

Table 2. Regression Parameters From the Hierarchical Linear Model Predicting Expected Smoking at Each Time Point

Region	Overall intercept	Slope of prior cravings	Moderation of craving slope by brain activation
Target regions			
Right IFG	0.51 (5.35)	0.24 (0.20)	−0.29* (0.12)
Left IFG	0.51 (4.64)	0.18 (0.15)	−0.23** (0.05)
Right pre-SMA	0.50 (5.60)	0.19 (0.18)	−0.20* (0.09)
Left pre-SMA	0.50 (5.45)	0.26* (0.12)	−0.23* (0.11)
Right basal ganglia	0.54 (4.96)	0.31* (0.14)	−0.27* (0.12)
Left basal ganglia	0.52 (4.99)	0.25* (0.12)	−0.32** (0.12)
Control regions			
Right amygdala	0.51 (5.22)	0.24* (0.11)	0.22* (0.09)
Left amygdala	0.50 (5.89)	0.16 (0.17)	0.03 (0.07)
Right precuneus	0.49 (5.82)	0.19 (0.20)	0.11 (0.08)
Left precuneus	0.50 (6.06)	0.19 (0.20)	0.11 (0.08)

Note: All parameters are reported in natural log units. Standard errors are given in parentheses. All models controlled for the linear decline in smoking across days, the negative quadratic pattern within days, and baseline nicotine dependence. IFG = inferior frontal gyrus; pre-SMA = pre-supplementary motor area.
*$p < .05$. **$p < .01$.

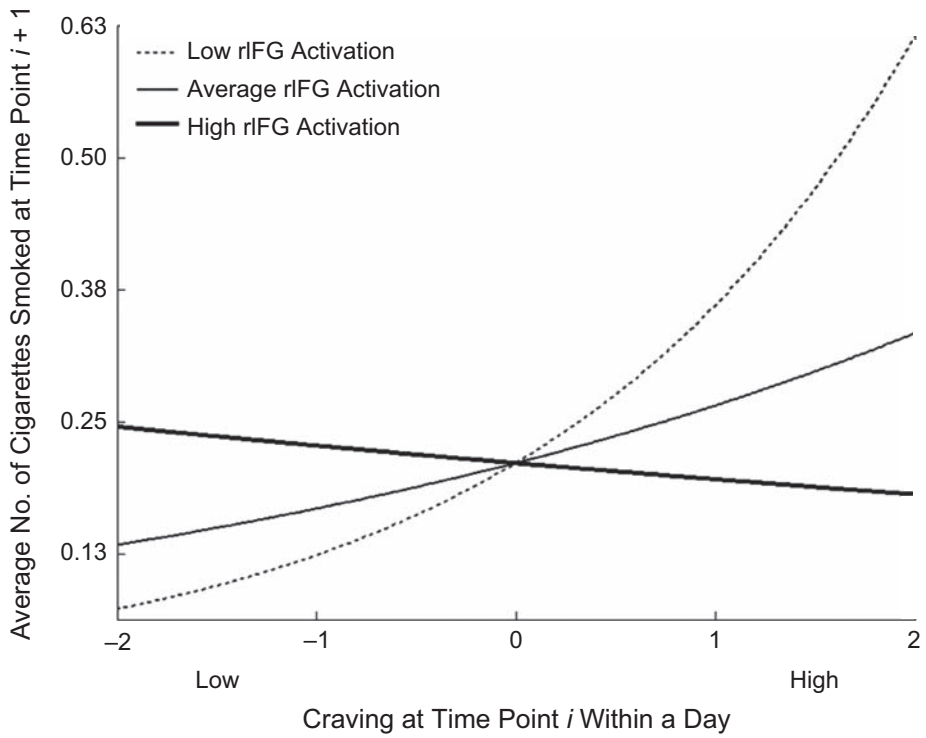

Fig. 4. Activation in right inferior frontal gyrus (rIFG) in the no-go > go contrast as a moderator of the relationship between cravings and subsequent smoking. The average number of cigarettes smoked at time *i* + 1 as a function of craving at time *i* is shown for participants with high (1 *SD* above the mean), average, and low (1 *SD* below the mean) rIFG activation in the contrast.

Discussion

This study investigated the neural underpinnings of the brief, recurring episodes of everyday self-control that are integral to successful goal pursuit. We employed a joint fMRI/experience-sampling approach to link neuroimaging and ecological methods (cf. Eisenberger, Gable, & Lieberman, 2007). The results support the notion that laboratory neurocognitive measures of response inhibition relate meaningfully to real-world instances of self-control. Activation in three regions that have been consistently associated with response inhibition in laboratory go/no-go tasks—rIFG, pre-SMA, and basal ganglia—was related to attenuating the link between cigarette craving and subsequent smoking. More generally, we demonstrated that neural activations moderated the relationship between two momentary measures acquired in the real world.

These results add to emerging evidence supporting the predictive power of brain-imaging data. In contrast to traditional approaches, in which brain activation is modeled as a dependent measure regressed on time-course variables, the *brain-as-predictor* approach employed here models brain activation as an independent measure that may account for unexplained variance in other outcomes (Bandettini, 2009). Variants of this approach have been used to classify participants' visual-system activation into two categories (Haxby et al., 2001) and to predict decision outcomes of individual participants given a set of four choices (Soon, Brass, Heinze, & Haynes, 2008). More recently, we built upon these findings by showing that neural activation during exposure to a persuasive message predicted health-behavior change a week later (Falk, Berkman, Mann, Harrison, & Lieberman, 2010). The present study extended the brain-as-predictor approach further still by demonstrating that brain-imaging data had between-subjects predictive validity regarding an important health behavior over a span of 4 weeks and within-subjects discriminant validity in predicting a fine-grained self-regulatory process.

The present study also has several substantive implications for understanding the neural systems involved in smoking cessation. Though the rIFG, pre-SMA, and basal ganglia had been implicated in previous laboratory studies of response inhibition (e.g., Wager et al., 2005), and response-inhibition performance in the laboratory had been associated with addiction outcomes (e.g., Monterosso et al., 2005), it remained unclear whether brief response inhibition during the laboratory task relies on the same neural systems as do more prolonged forms of response inhibition, such as regulation of cravings for cigarettes across a period of weeks. Here, we found that the extent of neural activation in stopping a prepotent motor response (i.e., no-go trials) was related to success at repeatedly preventing a habitual response (i.e., smoking). This suggests that some of the interventions that have been shown to improve response inhibition in the laboratory (e.g., Muraven,

2010) may also improve real-world forms of response inhibition (Berkman, Burklund, & Lieberman, 2009). Further, the fact that baseline activation in these regions was specifically related to the regulation of cravings on a daily basis hints at the diagnostic utility of neuroimaging data in smoking cessation. For example, it may be possible to develop tailored smoking-cessation programs targeting craving regulation in individuals with relatively low baseline response-inhibition capacity. It is important to note that response-inhibition capacity is only one of many neurocognitive skills that are likely to be critical to effective smoking cessation (see, e.g., Hare, Camerer, & Rangel, 2009, on the modulation of the ventromedial prefrontal cortex valuation system during self-control).

Among all three regions that were related to an attenuated link between craving and smoking, only the basal ganglia also predicted overall reductions in smoking across the 1st month of cessation. It may be that a broad network including bilateral IFG, pre-SMA, and basal ganglia is involved in discrete instances of response inhibition, such as regulation of momentary cravings, whereas a subset of this network or a distinct network (including basal ganglia and other regions) is involved in overall smoking change (see Supplemental Text in the Supplemental Material). To the extent that overall change in smoking involves not only response inhibition but also many other processes, it makes sense that a contrast that isolates only response-inhibition-related activity to the exclusion of other processes would not relate to global smoking change. It is possible that the basal ganglia are active across a more general set of processes because of their direct anatomical involvement in coordinating motor actions. This would be consistent with the finding that both the caudate and the putamen contributed to the attenuated craving-smoking link. In this view, it makes sense that the basal ganglia predict overall smoking change better than the other members of the response-inhibition network do, as activation of the latter regions may be more specific to response inhibition and less sensitive to other processes.

The present study represents a step toward increasing the integration of functional neuroimaging methods, such as fMRI, with ecological methods, such as experience sampling. We linked across neurocognitive and behavioral measures of response inhibition in the domain of smoking cessation; we investigated merely one process within one health-relevant domain. This research yielded valuable insights about the mechanisms of response inhibition that would otherwise have been difficult or impossible to obtain. Yet within the domain of smoking cessation, there are several other central processes (e.g., goal maintenance, attention regulation) whose investigation using these methods might yield equally valuable insights (Berkman & Lieberman, 2009). The present investigation highlights the benefits of this approach, including the ability to connect otherwise-decontextualized neuroimaging data to the real world and to probe the temporal extent of processes of interest, and paves the way for future research to capitalize on the potential for this approach to forge links across measurement modalities.

Acknowledgments

We are grateful to Naomi Eisenberger, Edythe London, Jane Mendle, and Steven Reise, as well as two anonymous reviewers, for helpful feedback on earlier drafts of this manuscript.

Declaration of Conflicting Interests

The authors declared that they had no conflicts of interest with respect to their authorship or the publication of this article.

Supplemental Material

Additional supporting information may be found at http://pss.sagepub.com/content/by/supplemental-data

References

Achtziger, A., Gollwitzer, P.M., & Sheeran, P. (2008). Implementation intentions and shielding goal striving from unwanted thoughts and feelings. *Personality and Social Psychology Bulletin*, *34*, 381–393.

Allen, S.S., Bade, T., Hatsukami, D., & Center, B. (2008). Craving, withdrawal, and smoking urges on days immediately prior to smoking relapse. *Nicotine & Tobacco Research*, *10*, 35–45.

Aron, A.R., Durston, S., Eagle, D.M., Logan, G.D., Stinear, C.M., & Stuphorn, V. (2007). Converging evidence for a fronto-basal-ganglia network for inhibitory control of action and cognition. *The Journal of Neuroscience*, *27*, 11860–11864.

Aron, A.R., Fletcher, P.C., Bullmore, E.T., Sahakian, B.J., & Robbins, T.W. (2003). Stop-signal inhibition disrupted by damage to right inferior frontal gyrus in humans. *Nature Neuroscience*, *6*, 115–116.

Aron, A.R., & Poldrack, R.A. (2006). Cortical and subcortical contributions to Stop signal response inhibition: Role of the subthalamic nucleus. *The Journal of Neuroscience*, *26*, 2424–2433.

Aron, A.R., Robbins, T.W., & Poldrack, R.A. (2004). Inhibition and the right inferior frontal cortex. *Trends in Cognitive Sciences*, *8*, 170–177.

Bandettini, P.A. (2009). What's new in neuroimaging methods? *Annals of the New York Academy of Sciences*, *1156*, 260–293.

Bauer, D.J., & Curran, P.J. (2005). Probing interactions in fixed and multilevel regression: Inferential and graphical techniques. *Multivariate Behavioral Research*, *40*, 373–400.

Berkman, E.T., Burklund, L., & Lieberman, M.D. (2009). Inhibitory spillover: Intentional motor inhibition produces incidental limbic inhibition via right inferior frontal cortex. *NeuroImage*, *47*, 705–712.

Berkman, E.T., & Lieberman, M.D. (2009). The neuroscience of goal pursuit: Bridging gaps between theory and data. In G. Moskowitz & H. Grant (Eds.), *The psychology of goals* (pp. 98–126). New York, NY: Guilford Press.

Biener, L., & Abrams, D.B. (1991). The contemplation ladder: Validation of a measure of readiness to consider smoking cessation. *Health Psychology*, *10*, 360–365.

Botvinick, M.M., Cohen, J.D., & Carter, C.S. (2004). Conflict monitoring and anterior cingulate cortex: An update. *Trends in Cognitive Sciences*, *8*, 539–546.

Chambers, C.D., Bellgrove, M.A., Stokes, M.G., Henderson, T.R., Garavan, H., Robertson, I.H., et al. (2006). Executive ''brake failure'' following deactivation of human frontal lobe. *Journal of Cognitive Neuroscience*, *18*, 444–455.

Eisenberger, N.I., Gable, S.L., & Lieberman, M.D. (2007). Functional magnetic resonance imaging responses relate to differences in real-world social experience. *Emotion*, *7*, 745–754.

Falk, E.B., Berkman, E.T., Mann, T., Harrison, B., & Lieberman, M.D. (2010). Predicting persuasion-induced behavior change from the brain. *The Journal of Neuroscience*, *30*, 8421–8424.

Finkel, E., DeWall, C., Slotter, E., Oaten, M., & Foshee, V. (2009). Self-regulatory failure and intimate partner violence perpetration. *Journal of Personality and Social Psychology*, *97*, 483–499.

Fuster, J.M. (2008). *The prefrontal cortex* (4th ed.). Boston, MA: Academic Press/Elsevier.

Hare, T.A., Camerer, C.F., & Rangel, A. (2009). Self-control in decision-making involves modulation of the vmPFC valuation system. *Science*, *324*, 646–648.

Haxby, J.V., Gobbini, M.I., Furey, M.L., Ishai, A., Schouten, J.L., & Pietrini, P. (2001). Distributed and overlapping representations of faces and objects in ventral temporal cortex. *Science*, *293*, 2425–2430.

Heatherton, T.F., Kozlowski, L.T., Frecker, R.C., & Fagerström, K.O. (1991). The Fagerström Test for nicotine dependence: A revision of the Fagerström Tolerance Questionnaire. *British Journal of Addiction*, *86*, 1119–1127.

Leung, H.-C., & Cai, W. (2007). Common and differential ventrolateral prefrontal activity during inhibition of hand and eye movements. *The Journal of Neuroscience*, *27*, 9893–9900.

Maldjian, J.A., Laurienti, P.J., Kraft, R.A., & Burdette, J.H. (2003). An automated method for neuroanatomic and cytoarchitectonic atlas-based interrogation of fMRI data sets. *NeuroImage*, *19*, 1233–1239.

Monterosso, J.R., Aron, A.R., Cordova, X., Xu, J., & London, E.D. (2005). Deficits in response inhibition associated with chronic methamphetamine abuse. *Drug and Alcohol Dependence*, *79*, 273–277.

Mostofsky, S.H., & Simmonds, D.J. (2008). Response inhibition and response selection: Two sides of the same coin. *Journal of Cognitive Neuroscience*, *20*, 751–761.

Muraven, M. (2010). Building self-control strength: Practicing self-control leads to improved self-control performance. *Journal of Experimental Social Psychology*, *46*, 465–468.

Nachev, P., Wydell, H., O'Neill, K., Husain, M., & Kennard, C. (2007). The role of the pre-supplementary motor area in the control of action. *NeuroImage*, *36*, T155–T163.

Nigg, J.T., Wong, M.M., Martel, M.M., Jester, J.M., Puttler, L.I., Glass, J.M., et al. (2006). Poor response inhibition as a predictor of problem drinking and illicit drug use in adolescents at risk for alcoholism and other substance use disorders. *Journal of the American Academy of Child and Adolescent Psychiatry*, *45*, 468–475.

Oaten, M., & Cheng, K. (2006). Improved self-control: The benefits of a regular program of academic study. *Basic and Applied Social Psychology*, *28*, 1–16.

Raudenbush, S.W., Bryk, A.S., Cheong, Y.F., & Congdon, R. (2004). *HLM6: Hierarchical linear and nonlinear modeling*. Lincolnwood, IL: Scientific Software International.

Rollnick, S., Heather, N., Gold, R., & Hall, W. (1992). Development of a short 'readiness to change' questionnaire for use in brief, opportunistic interventions among excessive drinkers. *British Journal of Addiction*, *87*, 743–754.

Rothman, A.J., Sheeran, P., & Wood, W. (2009). Reflective and automatic processes in the initiation and maintenance of dietary change. *Annals of Behavioral Medicine*, *38*, S4–S17.

Shiffman, S., Balabanis, M.H., Gwaltney, C.J., Paty, J.A., Gnys, M., Kassel, J.D., et al. (2007). Prediction of lapse from associations between smoking and situational antecedents assessed by ecological momentary assessment. *Drug and Alcohol Dependence*, *91*, 159–168.

Shiffman, S., Engberg, J.B., Paty, J.A., Perz, W.G., Gnys, M., Kassel, J.D., & Hickcox, M. (1997). A day at a time: Predicting smoking lapse from daily urge. *Journal of Abnormal Psychology*, *106*, 104–116.

Soon, C.S., Brass, M., Heinze, H.-J., & Haynes, J.-D. (2008). Unconscious determinants of free decisions in the human brain. *Nature Neuroscience*, *11*, 543–545.

Tiffany, S.T., & Drobes, D.J. (1991). The development and initial validation of a questionnaire on smoking urges. *British Journal of Addiction*, *86*, 1467–1476.

Tzourio-Mazoyer, N., Landeau, B., Papathanassiou, D., Crivello, F., Etard, O., Delcroix, N., & Mazoyer, M.J. (2002). Automated anatomical labeling of activations in SPM using a macroscopic anatomical parcellation of the MNI MRI single-subject brain. *NeuroImage*, *15*, 273–289.

Van Gaal, S., Ridderinkhof, K.R., Scholte, H.S., & Lamme, V.A.F. (2010). Unconscious activation of the prefrontal no-go network. *The Journal of Neuroscience*, *30*, 4143–4150.

Wager, T.D., Sylvester, C.-Y.C., Lacey, S.C., Nee, D.E., Franklin, M., & Jonides, J. (2005). Common and unique components of response inhibition revealed by fMRI. *NeuroImage*, *27*, 323–340.

Williams, L.M., Brown, K.J., Palmer, D., Liddell, B.J., Kemp, A.H., Olivieri, G., et al. (2006). The mellow years?: Neural basis of improving emotional stability over age. *The Journal of Neuroscience*, *26*, 6422–6430.

Wood, W., & Neal, D.T. (2007). A new look at habits and the habit-goal interface. *Psychological Review*, *114*, 843–863.

Supplemental Text for:

In the trenches of real-world self-control:

Neural correlates of breaking the link between craving and smoking

Elliot T. Berkman

University of Oregon

Emily B. Falk

University of Michigan

Matthew D. Lieberman

University of California, Los Angeles

Supplementary Methods

fMRI data acquisition and analysis

Participants were situated in the scanner, where foam padding was placed around their heads to reduce motion. Stimuli were presented on LCD goggles, and responses were recorded on a magnet-safe joystick placed in the right hand (Resonance Technology, Northridge, CA, USA). Participants responded to each go trial by pushing or pulling a lever then clicking a button at the top of the lever. Response time was computed as the latency between stimulus onset and the button click, errors were determined according to trial type, and distance and velocity were calculated based on the position of the lever at the time of the button click.

High-resolution structural T2-weighted echo-planar images (spin-echo; TR = 5000 ms; TE = 34 ms; matrix size 128 x 128; 34 sagittal slices; FOV = 192mm; 4 mm thick) were acquired coplanar with the functional scans. Four functional scans lasting 6:30, 5:46, 5:46 and 5:00 were acquired during the task (echo-planar T2*-weighted gradient-echo, TR = 2000 ms, TE = 30 ms, flip angle = 90°, matrix size 64 x 64, 34 axial slices, FOV = 192 mm; 4 mm thick), totaling 692 functional volumes.

The imaging data were analyzed using a combination of FSL tools (FMRIB Software Library; Oxford University, Oxford, UK) and SPM8 (Wellcome Department of Cognitive Neurology, Institute for Neurology, London, UK). The preprocessing stream for the images was as follows. All images were brain-extracted using BET (FSL's Brain Extraction Tool) and realigned within runs using MCFLIRT (FSL's Motion Correction using FMRIB's Linear Image Registration Tool), then checked for residual motion and noise spikes using a custom automated diagnostic tool (thresholded at 2mm motion or 2% global signal change from one image to the next). In SPM8, all functional and anatomical images were reoriented to set the origin to the

anterior commissure and the horizontal (*y*) axis parallel to the AC-PC line. Also in SPM8, functional images were corrected for slice acquisition timing differences within volumes, realigned within and between runs to correct for residual head motion, and coregistered to the matched-bandwidth structural scan using a 6-parameter rigid body transformation. The coregistered structural scan was then normalized into the Montreal Neurological Institute (MNI) standard stereotactic space and the resulting parameters were applied to all functional images. Finally, the normalized functional images were smoothed using an 8 mm full width at half maximum Gaussian kernel.

One run from each of two participants was removed due to motion. Data from three other participants contained motion spikes that were statistically removed using regressors corresponding to the affected scans.

The design was modeled as an event-related within-subjects one-way ANOVA with response inhibition as a factor with two levels: go and no-go. An implicit baseline condition was comprised of the twelve-second fixation periods that followed each block. Each trial was modeled as an event with 1-second duration and convolved with the canonical hemodynamic response. Temporal autocorrelations in the functional data were addressed using a first-order auto-regressive error structure.

We used a Monte Carlo simulation (AlphaSim; distributed as part of the AFNI Software Package, Medical College of Wisconsin, Milwaukee, WI) to determine that the minimum cluster size necessary to maintain a false detection rate of 5% for a whole-brain search of the [no-go > go] contrast was 20 3x3x3mm voxels combined with a voxel-wise threshold of .001. All functional imaging results are reported in MNI coordinates.

Experience sampling

Participants could silence or disable their phones at their discretion. In the event that they were unable to respond to a prompt before the arrival of the subsequent prompt they were instructed to respond only to the most recent prompt. In other words, participants had roughly two hours to respond to each prompt. Participants were sent a reminder text message or received a phone call if their response rate dropped below 50% for a 24-hour period.

The text message prompts were sent and received through an automated web-based service (RedOxygen Pty. Ltd., Brisbane, Queensland, Australia). Records including the timestamp and content of each message that was sent and received were downloaded from the RedOxygen website.

The Freedom From Smoking cessation program was ongoing from two weeks before the quit date until six weeks following the quit date. Thus, all participants were enrolled in the program for the entire duration of the experience sampling phase of the study.

Time-series data often violates the assumption of sphericity among the dependent measures. To test for this, we used the Hierarchical Multivariate Linear Modeling module of HLM6 to run a nested set of models. The most unrestricted model allowed for all separate variances and covariances within the 8x8 within-day variance-covariance matrix, and more restrictive variance structures such as identical variances but unique covariances and first-order auto-regressive were nested within that model. Deviance change tests suggested that sphericity was met within-days. Nonetheless, we used robust estimates of standard errors with the assumption of over-dispersion to conservatively guard against violations of normality and sphericity (Zeger, Liang, & Albert, 1988).

Integration of fMRI and experience sampling data

To assess which inhibition-related neural activations had prospective predictive value of smoking cessation outcomes, we identified voxels that correlated with overall smoking change from baseline to endpoint within a functional ROI based on significant activations in the no-go > go contrast. This is a relatively conservative approach because these voxels will have reduced variance due to their restricted range (Lieberman, Berkman, & Wager, 2009). False detection rate of .05 was achieved on this analysis using a combined voxel-wise threshold of .01 for each of the conjoined analyses together with a cluster-extent threshold of 20 voxels (Kampe, Frith, & Frith, 2003; Ochsner, Hughes, Robertson, Cooper, & Gabrieli, 2009). To further bolster the predictive power by testing their generalizability to new data, results from this analysis were entered into a leave-one-out cross-validation analysis (Falk, Berkman, Mann, Harrison, & Lieberman, 2010; Stone, 1974). This analysis identified regions in which activation during response inhibition at baseline was predictive of subsequent global success at smoking cessation across a four-week period.

Supplementary Results

Smoking change from baseline to endpoint

Within days, there was a positive relationship between craving at one time point and smoking at the next when craving was entered alone into the model (i.e. without neural activations; log-expectation $\gamma = .19$, $SE = .08$, $t(476) = 2.14$, $p < .05$). Individuals in the upper tertile of this everyday craving-smoking relationship (i.e. those with a strong positive relationship) reduced smoking significantly less (M= 8.50 cigarette reduction/day) than those in the lower tertile (i.e. those with a weak or no relationship between craving and smoking; M=18.44 cigarette reduction/day, $t_{24}=2.22$, $p<.05$).

Predicting everyday response inhibition from neuroimaging data

To explore the differential contributions of the caudate and putamen within the basal ganglia, we ran the analysis separately for left and right ROIs of each of those regions based on the AAL toolbox (Tzourio-Mazoyer, et al., 2002). Activation in the left caudate (log-γ = -.20, p<.04) and the left and right putamen (log-γs = -.17, -.21, ps<.05) moderated the link between craving and smoking. The right caudate slope (log-γ = -.16) was not significantly different from the left caudate slope, but did not meet our significance threshold (p<.14). Together, activation in the bilateral basal ganglia during response inhibition significantly moderated the relationship between craving and smoking (see Table 2).

We ran another set of models to test whether the moderation of the craving-smoking link by activation in the ROIs was higher at greater levels of craving compared to lower levels of craving. To do this, we created a variable that coded for whether cravings were high (3 or 4 out of 4) or low (0, 1 or 2 out of 4), then generated the interaction term between mean-centered versions of this variable and the reports of prior craving. Conceptually, the slope between this variable and smoking tests whether high levels of craving were more related to smoking than low levels of craving. We then tested whether this interaction variable was significantly moderated by activation in our ROIs, conceptually testing whether the moderation of the craving-smoking link by brain activation was moderated by whether cravings were high or low. The results of these tests support the notion that the moderation of the craving-smoking link by neural activation was higher at relatively higher levels of craving: the moderation was significantly greater at high levels of craving (compared to low levels) for all six ROIs (all γs > .2, all p<.05).

Predicting global smoking change from neuroimaging data

We used a functional localizer to identify voxels associated with response inhibition (i.e. [no-go > go]), then searched within these for voxels that were also associated with change in

exhaled carbon monoxide. The only regions that survived this analysis were two clusters in the right basal ganglia, one cluster in the fusiform gyrus, and one cluster on the occipital pole (Table S1; Figure S1). A leave-one-out cross-validation procedure was used to extend the generalizability of this result to new samples. In this procedure, each participant's change in CO from baseline to endpoint was predicted from his or her right basal ganglia activation in [no-go > go] based on a linear statistical model from all other participants. Across iterations, there was a significant positive correlation between predicted and actual CO change, suggesting predictive validity in the neuroimaging data (cross-validated $r = .40$, $R^2 = 16\%$, $p < .05$; Figure S2).

Robustness to missing data

It seems possible that smokers attempting to quit might under-report smoking lapses, thus it is important to check that this potential systematic bias in the missing data (i.e missing not-at-random) does not affect the results. To check the robustness of our data, we generated simulated data under varying degrees of the assumption that participants systematically smoked more when they missed a smoking report. We simulated the data by computing the mean and standard deviation of daily smoking per participant and replaced instances of missing data with these imputed data. We note that this is a highly conservative test of the possibility of under-reporting of smoking because it assumes that each instance of missing data was counted as a lapse. Even if attempting quitters tended to under-report lapses, it still is unlikely that every missed report corresponded to a lapse.

We re-computed the parameter estimates for each of the key ROIs (IFG, preSMA, and basal ganglia) assuming that participants did not smoke more during missed responses compared to completed responses (mean), participants smoked slightly more during missed responses compared to completed responses (+1 SD), and participants smoked significantly more during

missed responses (+2 SD). In every case, the parameter estimates are slightly attenuated though still significant when missing data are imputed with mean, moderate, and high smoking. None of the parameter estimates fall below our significance threshold of $p<.05$, and none change significantly from the value reported in Table 2.

Also, the hypothesis that the parameter estimates are robust to this violation is further supported by the fact that the mean craving at time points immediately prior to completed responses (M=1.73) is not significantly different from the mean craving at time points immediately prior to missed responses (M=1.72, $p>.7$). Both of these analyses demonstrate that missing data did not impact the slope between craving and subsequent smoking.

Supplementary Discussion

Of our three ROIs commonly involved in response inhibition, only basal ganglia activation predicted long-term success in smoking cessation, but all three predicted successful outcomes of the smaller everyday battles between craving and self-control. And the outcomes of these battles—the battles to prevent craving becoming smoking—in turn related to the outcome of the war in terms of overall daily cigarette reduction. The role of rIFG and SMA in these struggles would have been lost if we had only examined the link between neural activation and overall success.

References

Falk, E. B., Berkman, E. T., Mann, T., Harrison, B., & Lieberman, M. D. (2010). Predicting persuasion-induced behavior change from the brain. *Journal of Neuroscience*, 1-21.

Kampe, K. K. W., Frith, C. D., & Frith, U. (2003). "Hey John": signals conveying communicative intention toward the self activate brain regions associated with "mentalizing," regardless of modality. *Journal of Neuroscience, 23*(12), 5258-5263.

Lieberman, M., Berkman, E. T., & Wager, T. (2009). Correlations in Social Neuroscience Aren't Voodoo: Commentary on Vul et al.(2009). *Perspectives on Psychological Science, 4*(3), 299-307.

Ochsner, K. N., Hughes, B., Robertson, E. R., Cooper, J. C., & Gabrieli, J. D. E. (2009). Neural Systems Supporting the Control of Affective and Cognitive Conflicts. *Journal of cognitive neuroscience, 21*(9), 1841-1854.

Stone, M. (1974). Cross-validation choice and assessment of statistical predictions. *Journal of the Royal Statistical Society B, 36*(2), 111-147.

Tzourio-Mazoyer, N., Landeau, B., Papathanassiou, D., Crivello, F., Etard, O., Delcroix, N., et al. (2002). Automated anatomical labeling of activations in SPM using a macroscopic anatomical parcellation of the MNI MRI single-subject brain. *Neuroimage, 15*(1), 273-289.

Zeger, S. L., Liang, K.-Y., & Albert, P. S. (1988). Models for longitudinal data: A generalized estimating equation approach. *Biometrics, 44*(4), 1049-1060.

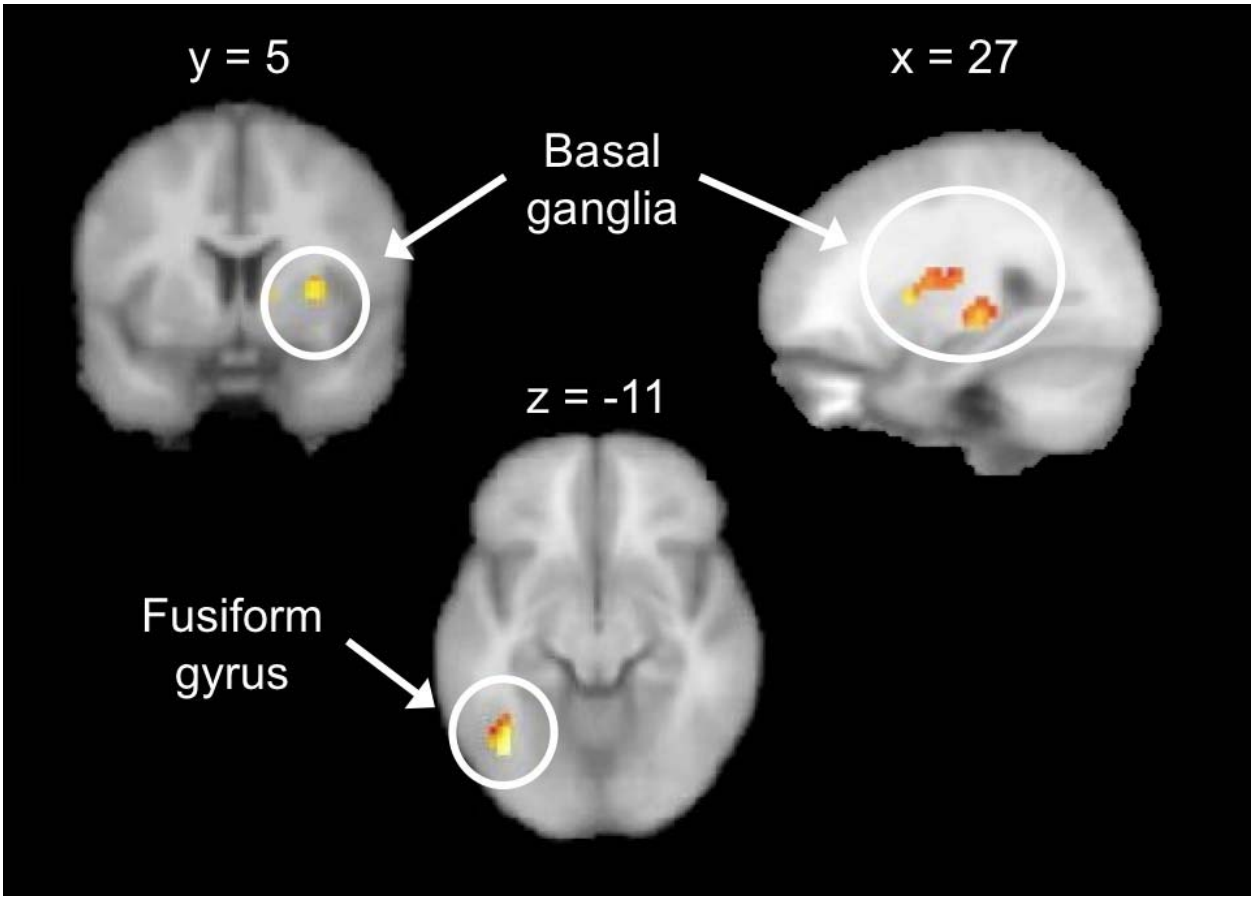

Figure S1. Regions active during the contrast of no-go > go that also correlated with global smoking change (CO from baseline to endpoint). These included the basal ganglia (top; peak MNI: 30 5 4), fusiform gyrus (bottom; -39 -64 -11), and occipital pole (not shown). All activations are FDR corrected at .05.

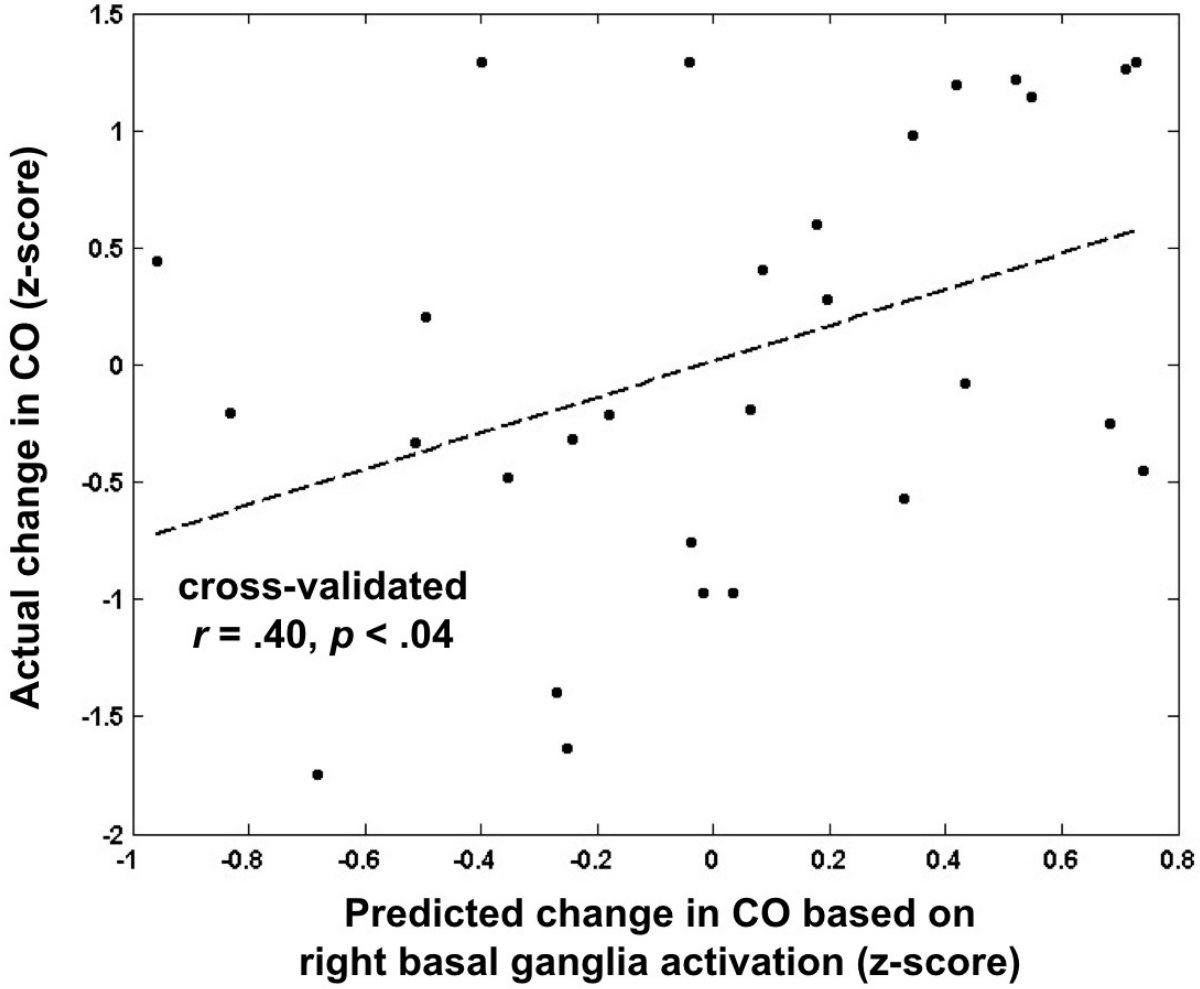

Figure S2. Correlation between actual exhaled carbon monoxide change (from baseline to endpoint) and predictions of change based on neural activation. Iterative leave-one-out cross-validated $r = .40$, $p < .04$.

Table S1

Regions active during [no-go > go] that correlated with change in exhaled CO

Effect	Region	x	y	z	Cluster size	t-val
No-go > go &	Basal ganglia	30	5	4	86	5.02
Positive correlation		30	-16	-2	53	5.78
	Fusiform gyrus	-39	-64	-11	20	6.64
	Occipital pole	-24	-94	10	20	7.57
No-go > go &	*None*					
Negative correlation						

Note. *N*=27. All regions FDR corrected at .05.